Supporting Information

Cyanogramide with a New Spiro[indolinone-pyrroloimidazole] Skeleton from *Actinoalloteichus cyanogriseus*

Peng Fu,[†] Fandong Kong,[†] Xia Li,[‡] Yi Wang,[†] and Weiming Zhu[*,†]

[†]Key Laboratory of Marine Drugs, Ministry of Education of China, School of Medicine and Pharmacy, Ocean University of China, Qingdao 266003, China; [‡]Marine College, Shandong University at Weihai, Weihai 264209, China

List of Supporting Information

Experimental details

General Experimental Procedures. Specific rotations were obtained on a JASCO P-1020 digital polarimeter. UV spectra were recorded on Beckman DU 640 spectrophotometer. CD spectra were measured on JASCO J-715 spectropolarimeter. IR spectra were taken on a Nicolet Nexus 470 spectrophotometer in KBr discs. NMR spectra were recorded on a JEOL JNM-ECP 600 spectrometer using TMS as internal standard, and chemical shifts were recorded as δ values. ESIMS utilized on a Q-TOF Ultima Global GAA076 LC mass spectrometer. Semiprepartive HPLC was performed using an ODS column [YMC-pak ODS-A, 10 × 250 mm, 5 μm, 4 mL/min]. TLC and column chromatography (CC) were performed on plates precoated with silica gel GF_{254} (10–40 μm) and over silica gel (200–300 mesh, Qingdao Marine Chemical Factory), and Sephadex LH-20 (Amersham Biosciences), respectively. Vacuum-liquid chromatography (VLC) was carried out over silica gel H (Qingdao Marine Chemical Factory). Sea salt used is made from the evaporation of sea water collected in Laizhou Bay (Weifang Haisheng Chemical Factory).

Actinomycete Material, Fermentation and Extraction. The details of these parts were the same as those in references 9 and 10 of the text.

Purification. The gum (28.0 g) was separated into ten fractions on a silica gel VLC column using step gradient elution with CH_2Cl_2–petroleum ether (50%–100%) and then with MeOH–CH_2Cl_2 (0–50%). Fraction 2 (1.4 g) was separated into four subfractions by chromatography on a C_{18} column using stepwise gradient elution with 5–90% MeOH/H_2O. Subfraction 2-3 (90 mg) was further purified by semipreparative HPLC (70% MeOH–H_2O, 4.0 mL/min) to yield **1** (15 mg, t_R 10.9 min).

Multidrug resistance reversal assay. The ability of the compound to potentiate adriamycin or vincristine cytotoxicity was evaluated in K562/A02, MCF-7/Adr and KB/VCR cells by the MTT assay. Cells were seeded into 96-well plates at 2×10^4/well. Various concentrations of the test compound **1** and adriamycin or vincristine were subsequently added and incubated for 48 h. The IC_{50} values for compound **1** and adriamycin or vincristine (concentration resulting in 50% inhibition of cell growth) were calculated from plotted results using untreated cells as 100%. The reversal fold (RF) values, as potency of reversal, were obtained from fitting the data to RF = IC_{50} of cytotoxic drug alone/IC_{50} of cytotoxic drug in the presence of compound **1**.

Theory and Calculation Details. The calculations were performed by using the density functional theory (DFT) as carried out in the Gaussian 03.[S1] The preliminary conformational distributions search was performed by HyperChem 7.5 software. All ground-state geometries were optimized at the B3LYP/6-31G(d) level. Solvent effects of methanol solution were evaluated at the same DFT level by using the SCRF/PCM method.[S2] TDDFT[S3] at B3LYP/6-31G(d) was employed to calculate the electronic excitation energies and rotational strengths in methanol. The stable conformations obtained at the B3LYP/6-31G(d) level were further used in magnetic shielding constants at the B3LYP/6-311++G(2d,p) level.

Table S1. The calculated ^{13}C NMR data for (1*R*,12*R*)-**1** and (1*R*,12*S*)-**1**

position	measured **1**	Calcd.(1*R*, 12*R*)-**1**	Corr. (1*R*,12*R*)-**1**	Error	Calcd. (1*R*,12*S*)-**1**	Corr. (1*R*,12*S*)-**1**	Error
1	69.8	77.2	72.9	-3.1	77.5	73.8	-4.0
2	124.6	132.6	125.8	-1.2	132.2	125.6	-1.0
3	124.5	130.0	123.3	1.2	130.0	123.5	1.0
4	123.1	127.8	121.2	1.9	128.1	121.7	1.4
5	130.1	135.9	128.9	1.2	136.3	129.5	0.6
6	109.6	113.9	107.9	1.7	113.5	107.9	1.7
7	144.8	152.9	145.1	-0.3	152.8	145.1	-0.3
9	169.5	177.8	168.9	0.6	177.8	168.8	0.7
10	167.4	177.6	168.7	-1.3	178.5	169.5	-2.1
12	98.7	106.6	101.0	-2.3	107.0	101.7	-3.0
14	154.6	162.1	153.9	0.7	160.4	152.3	2.3
15	138.6	147.8	140.3	-1.7	147.4	140.0	-1.4
16	107.2	114.2	108.2	-1.0	115.3	109.6	-2.4
17	21.8	21.5	19.8	2.0	18.7	18.1	3.7
1'	118.9	127.2	120.6	-1.7	125.3	119.1	-0.2
2'	118.0	126.6	120.0	-2.0	123.7	117.5	0.5
3'	135.5	143.8	136.5	-1.0	143.3	136.1	-0.6
4'	126.1	126.8	120.2	5.9	127.4	121.1	5.0
5'	128.8	134.2	127.3	1.5	134.7	128.0	0.8
6'	127.6	132.3	125.5	2.1	132.8	126.2	1.4
7'	128.8	134.6	127.7	1.1	134.3	127.6	1.2
8'	126.1	135.5	128.5	-2.4	135.3	128.5	-2.4
8-NCH_3	26.9	26.9	24.9	2.0	26.9	25.8	1.1
12-OCH_3	49.4	56.5	53.2	-3.8	56.0	53.4	-4.0

References.

(S1) Gaussian 03, Revision E.01, M. J. Frisch, G. W. Trucks, H. B. Schlegel, G. E. Scuseria, M. A. Robb, J. R. Cheeseman, J. A. Montgomery, Jr., T. Vreven, K. N. Kudin, J. C. Burant, J. M. Millam, S. S. Iyengar, J. Tomasi, V. Barone, B. Mennucci, M. Cossi, G. Scalmani, N. Rega, G. A. Petersson, H. Nakatsuji, M. Hada, M. Ehara, K. Toyota, R. Fukuda, J. Hasegawa, M. Ishida, T. Nakajima, Y. Honda, O. Kitao, H. Nakai, M. Klene, X. Li, J. E. Knox, H. P. Hratchian, J. B. Cross, V. Bakken, C. Adamo, J. Jaramillo, R. Gomperts, R. E. Stratmann, O. Yazyev, A. J. Austin, R. Cammi, C. Pomelli, J. W. Ochterski, P. Y. Ayala, K. Morokuma, G. A. Voth, P. Salvador, J. J. Dannenberg, V. G. Zakrzewski, S. Dapprich, A. D. Daniels, M. C. Strain, O. Farkas, D. K. Malick, A. D. Rabuck, K. Raghavachari, J. B. Foresman, J. V. Ortiz, Q. Cui, A. G. Baboul, S. Clifford, J. Cioslowski, B. B. Stefanov, G. Liu, A. Liashenko, P. Piskorz, I. Komaromi, R. L. Martin, D. J. Fox, T. Keith, M. A. Al-Laham, C. Y. Peng, A. Nanayakkara, M. Challacombe, P. M. W. Gill, B. Johnson, W. Chen, M. W. Wong, C. Gonzalez, and J. A. Pople, Gaussian, Inc., Wallingford CT, 2004.

(S2) (a) Miertus, S.; Tomasi, J. *Chem. Phys.* **1982**, *65*, 239–245. (b) Tomasi, J.; Persico, M. *Chem. Rev.* **1994**, *94*, 2027–2094. (c) Cammi, R.; Tomasi, J. *J. Comp. Chem.* **1995**, *16*, 1449–1458.

(S3) (a) Casida, M. E. In Recent Advances in Density Functional Methods, part I; Chong, D. P., Eds.; World Scientific: Singapore, 1995; pp 155–192. (b) Gross, E. K. U.; Dobson, J. F.; Petersilka, M. Top. *Curr. Chem.* **1996**, *181*, 81–172. (c) Gross, E. K. U.; Kohn, W. Adv. Quantum Chem. **1990**, *21*, 255–291. (d) Runge, E.; Gross, E. K. U. *Phys. Rev. Lett.* **1984**, *52*, 997–1000.

Figure S1. Q-TOF-MS^2 spectrum of cyanogramide (**1**)

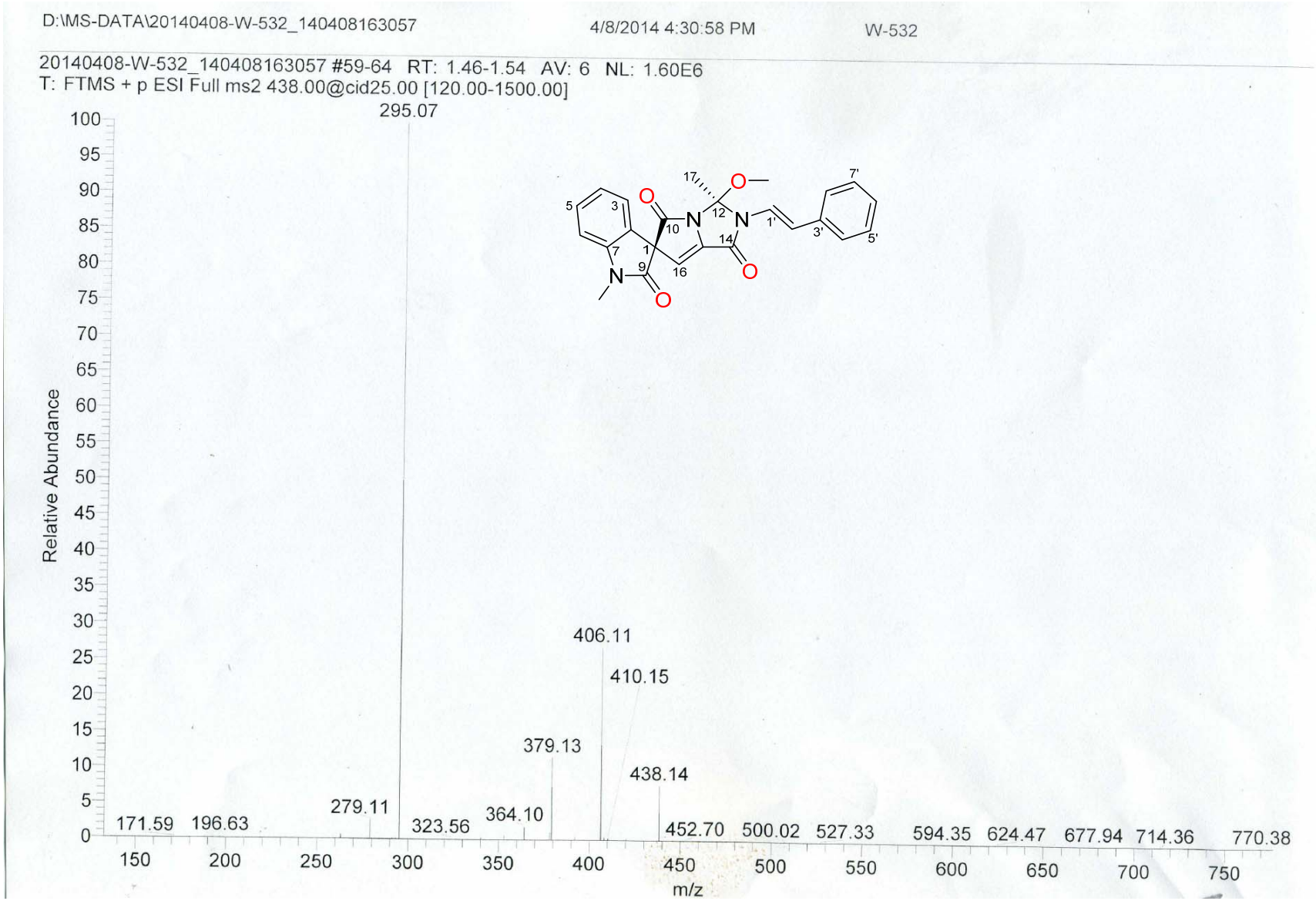

Figure S2. The ^{1}H-NMR spectrum of cyanogramide (**1**) in DMSO-d_6

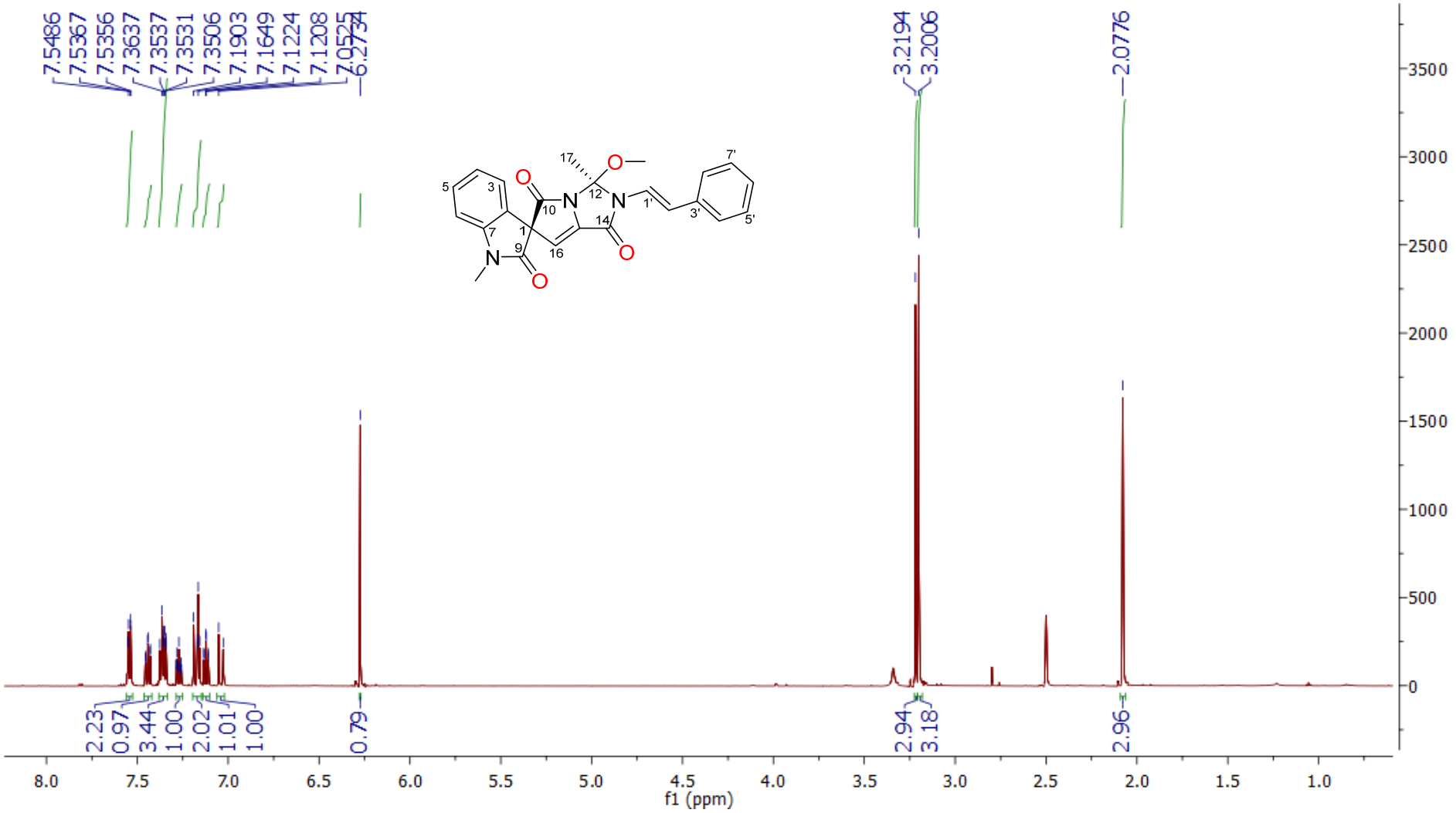

Figure S3. Expansion of ^{1}H-NMR spectrum of cyanogramide (**1**) in DMSO-d_6

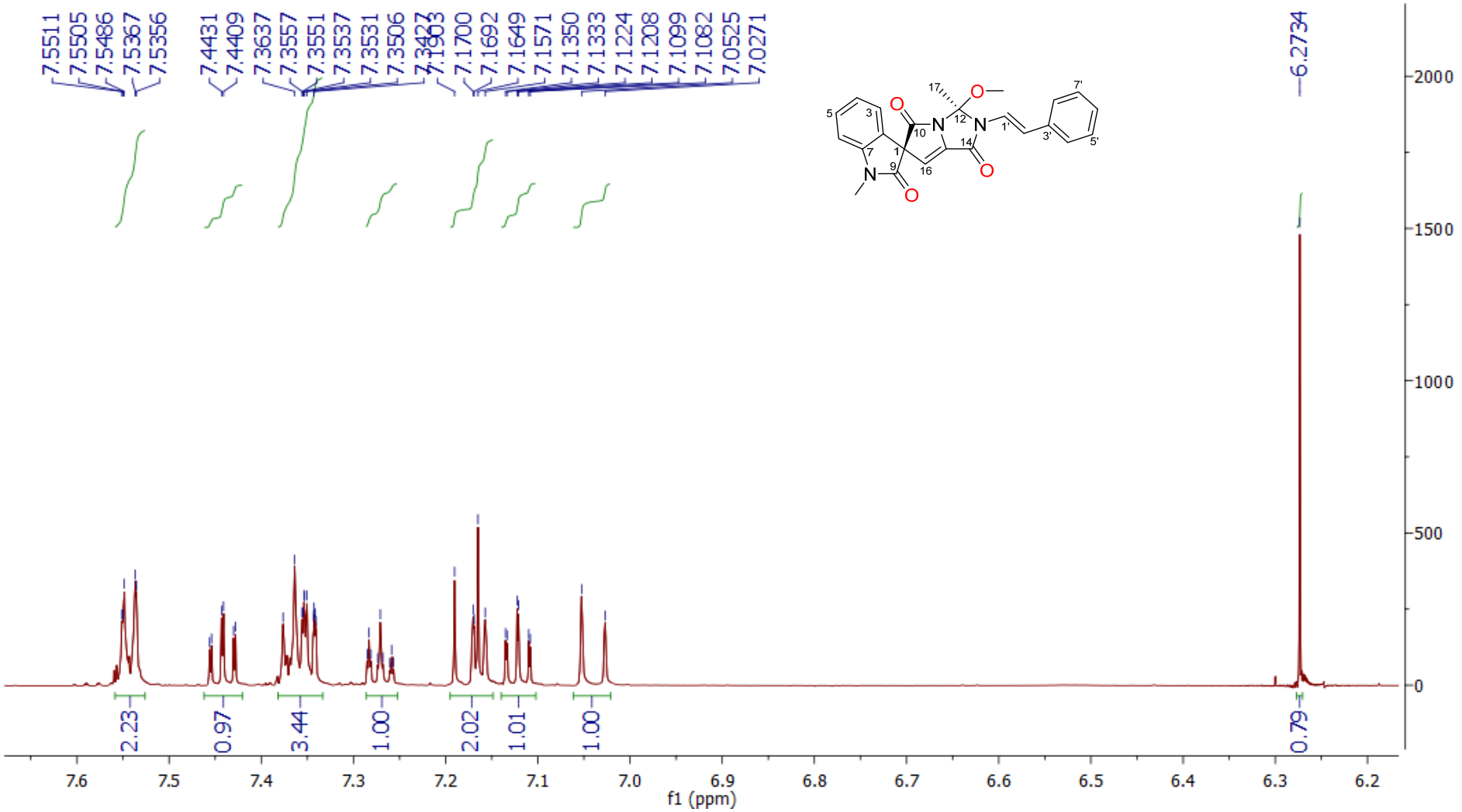

Figure S4. The ^{13}C-NMR spectrum of cyanogramide (**1**) in DMSO-d_6

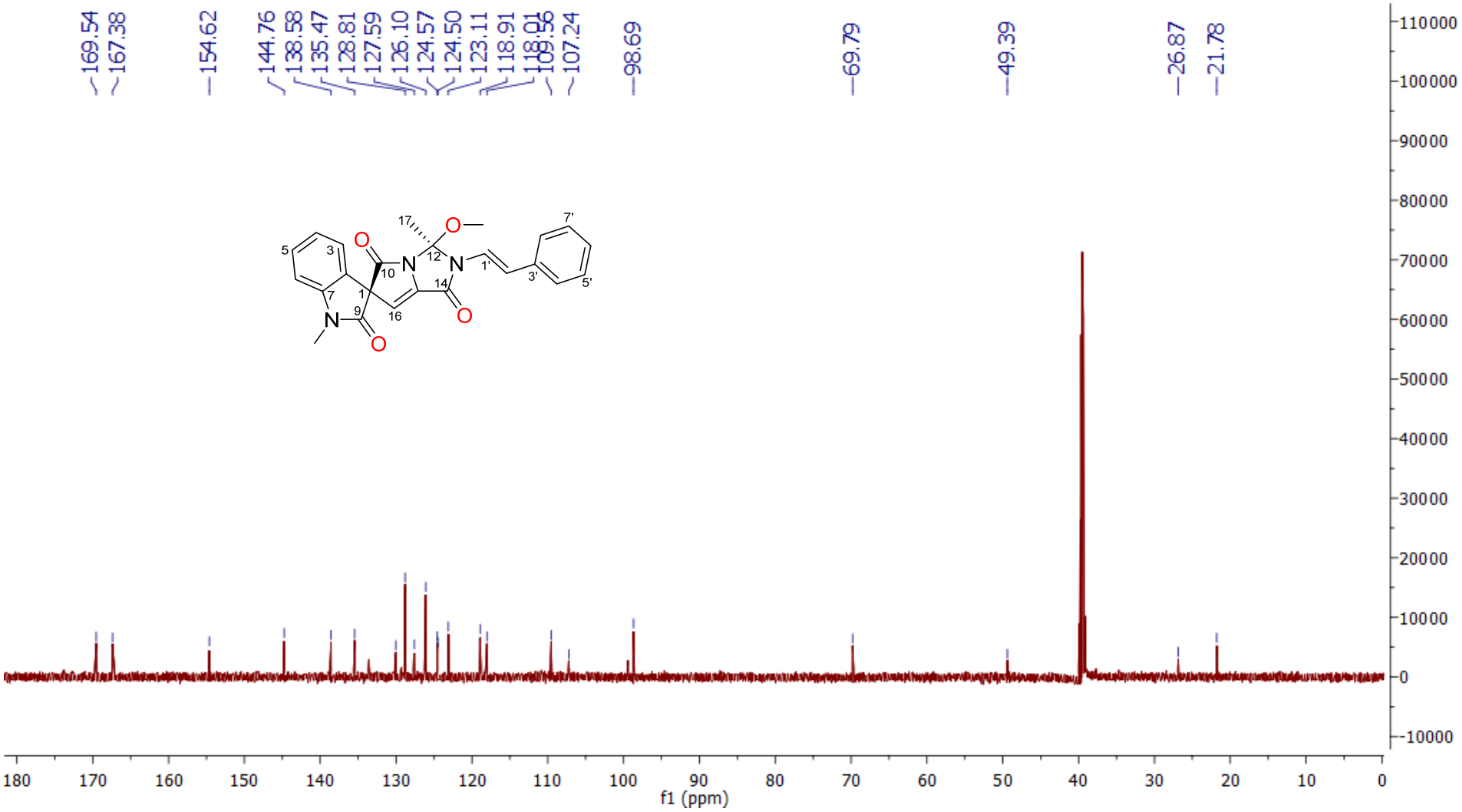

Figure S5. The DEPT spectrum of cyanogramide (**1**) in DMSO-d_6

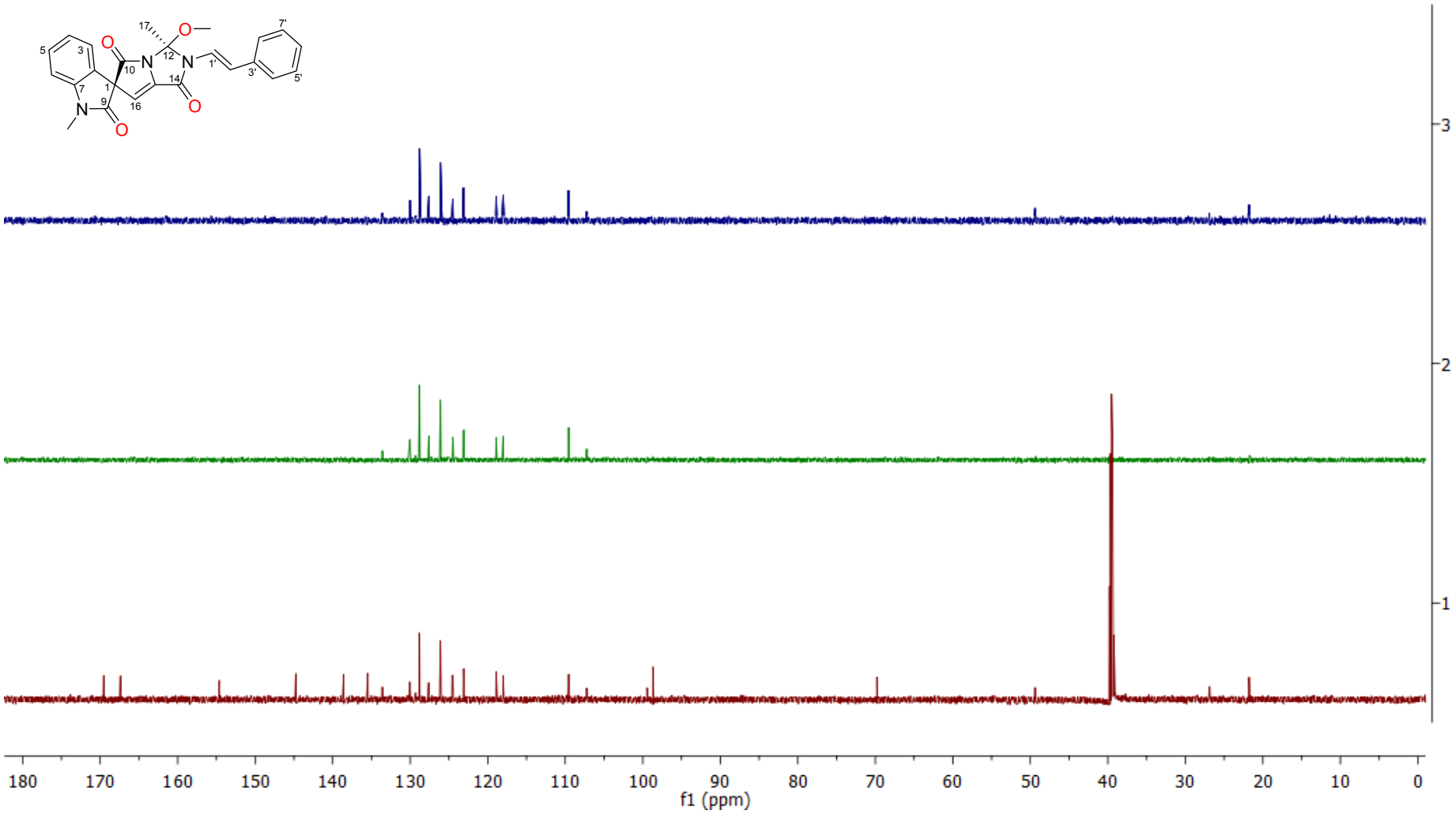

Figure S6. The HMQC spectrum of cyanogramide (**1**) in DMSO-d_6

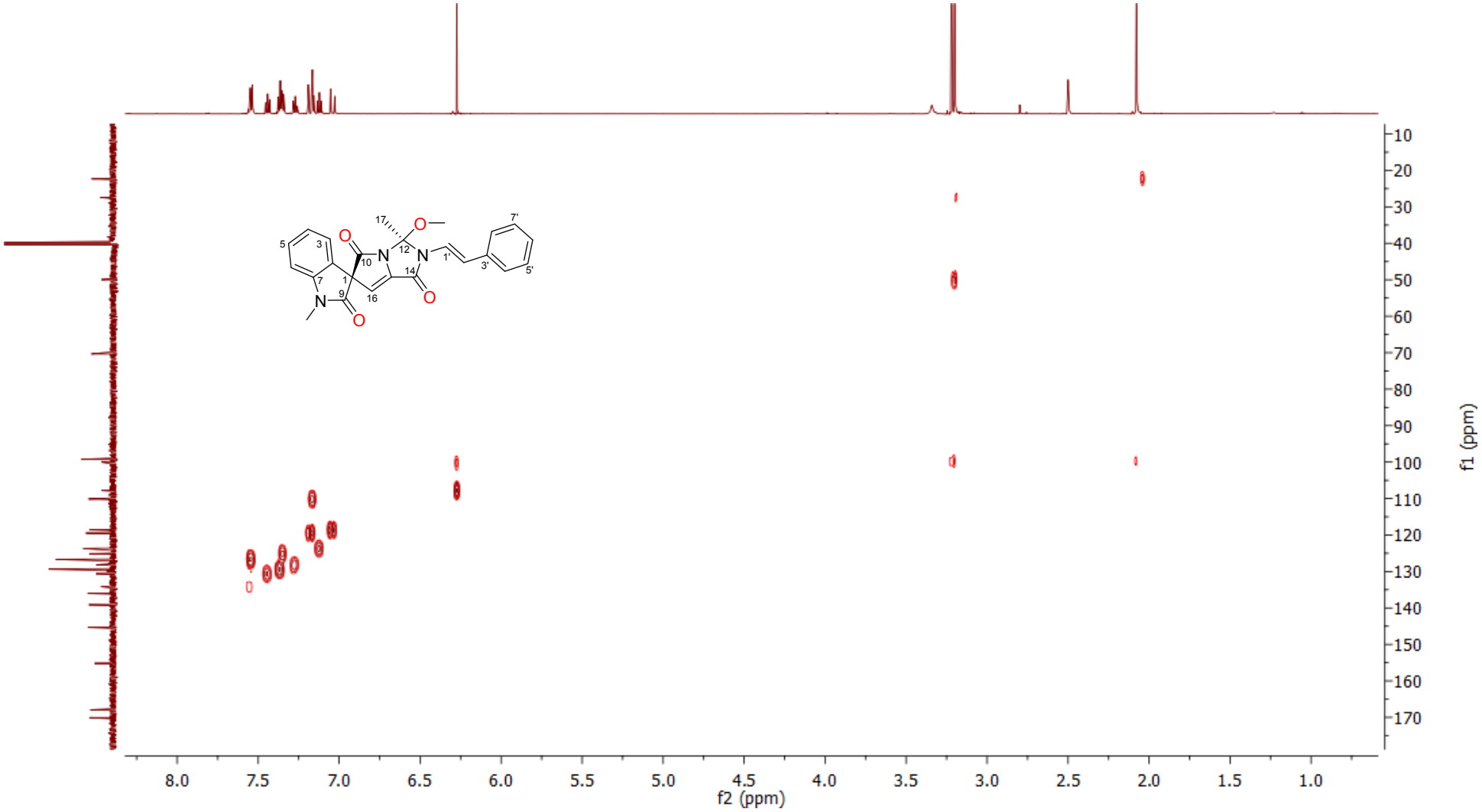

Figure S7. Expansion of HMQC spectrum of cyanogramide (**1**) in DMSO-d_6

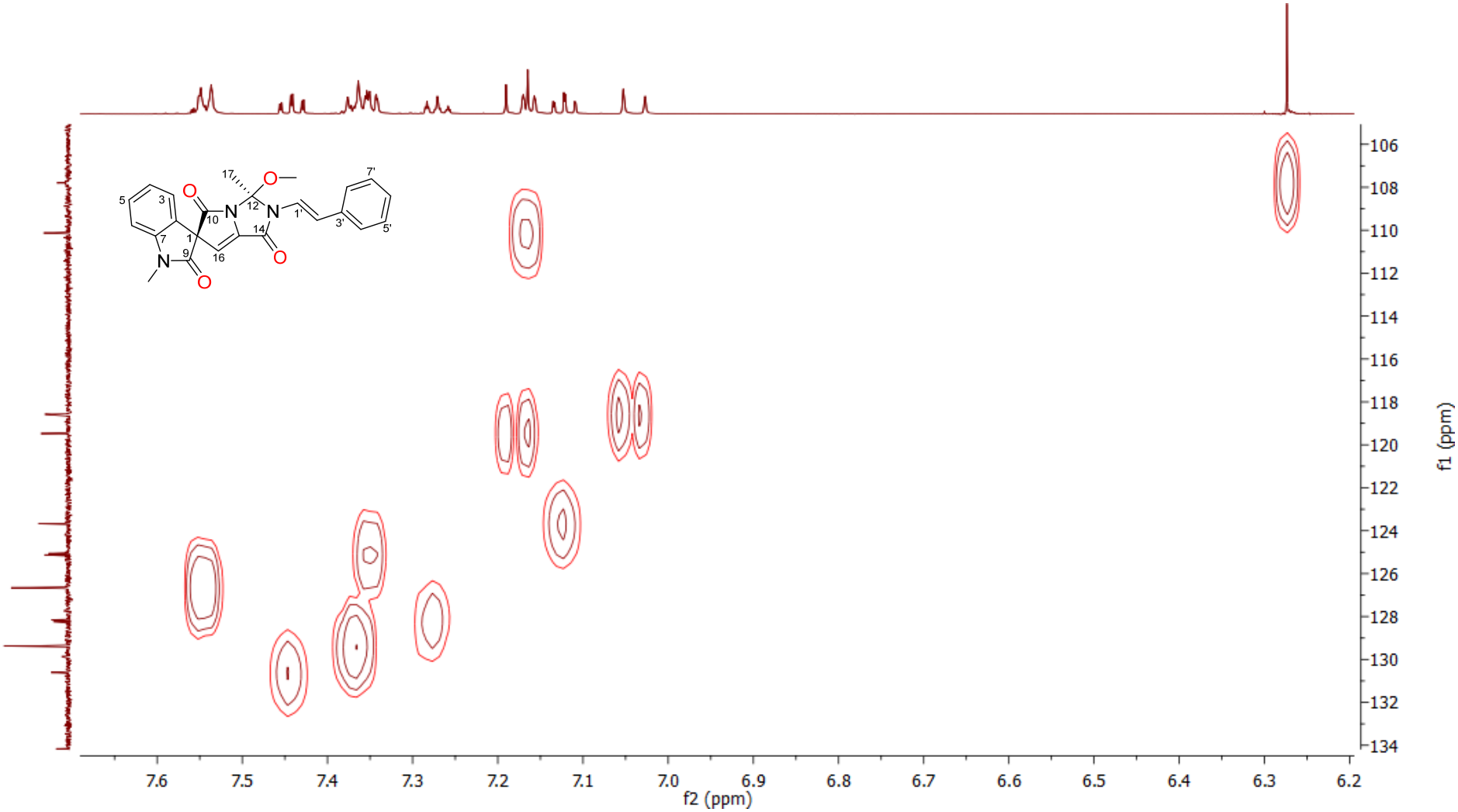

Figure S8. The ^{1}H-^{1}H COSY spectrum of cyanogramide (**1**) in DMSO-d_6

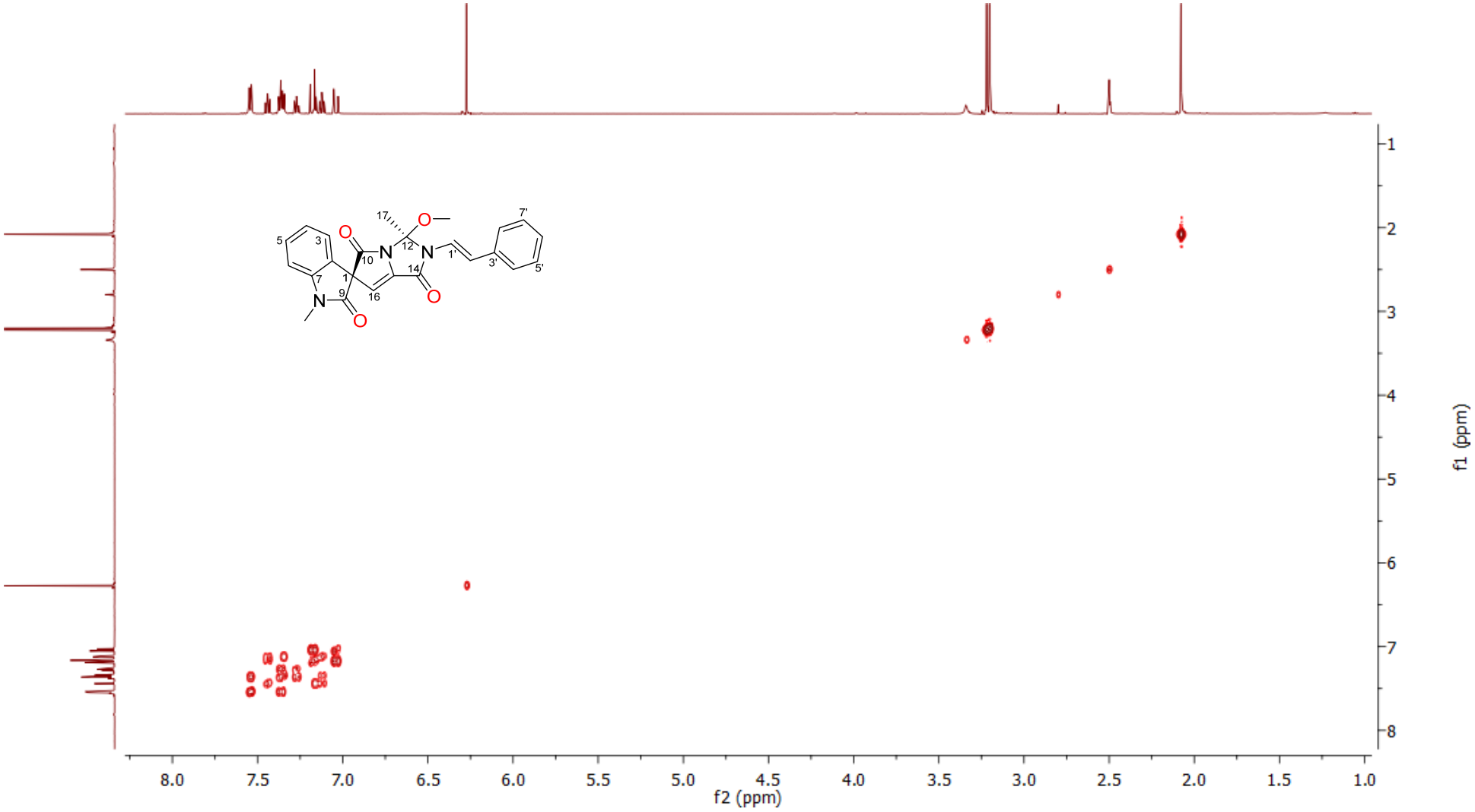

Figure S9. Expansion of ^{1}H-^{1}H COSY spectrum of cyanogramide (**1**) in DMSO-d_6

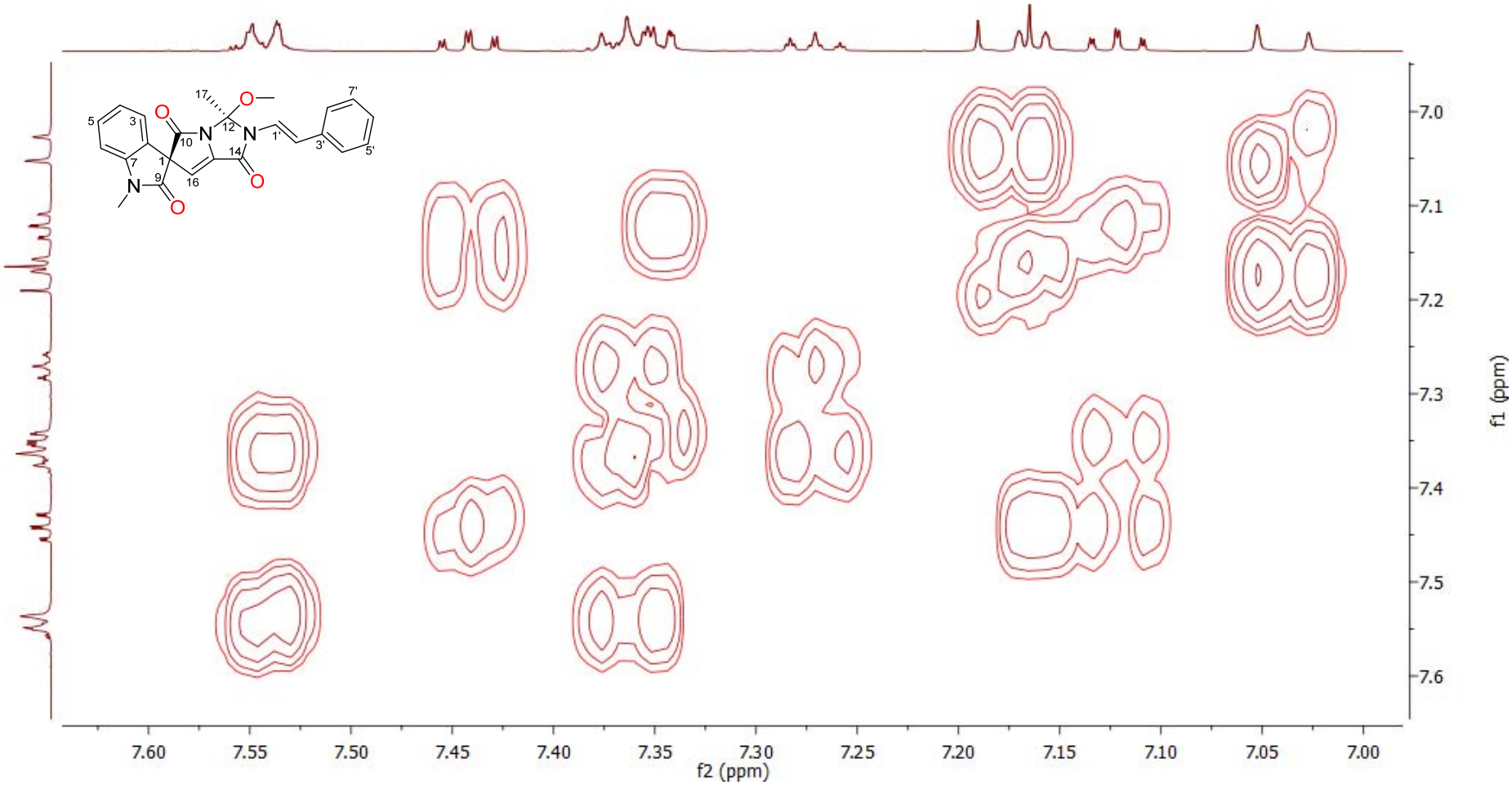

Figure S10. The HMBC spectrum of cyanogramide (**1**) in DMSO-d_6

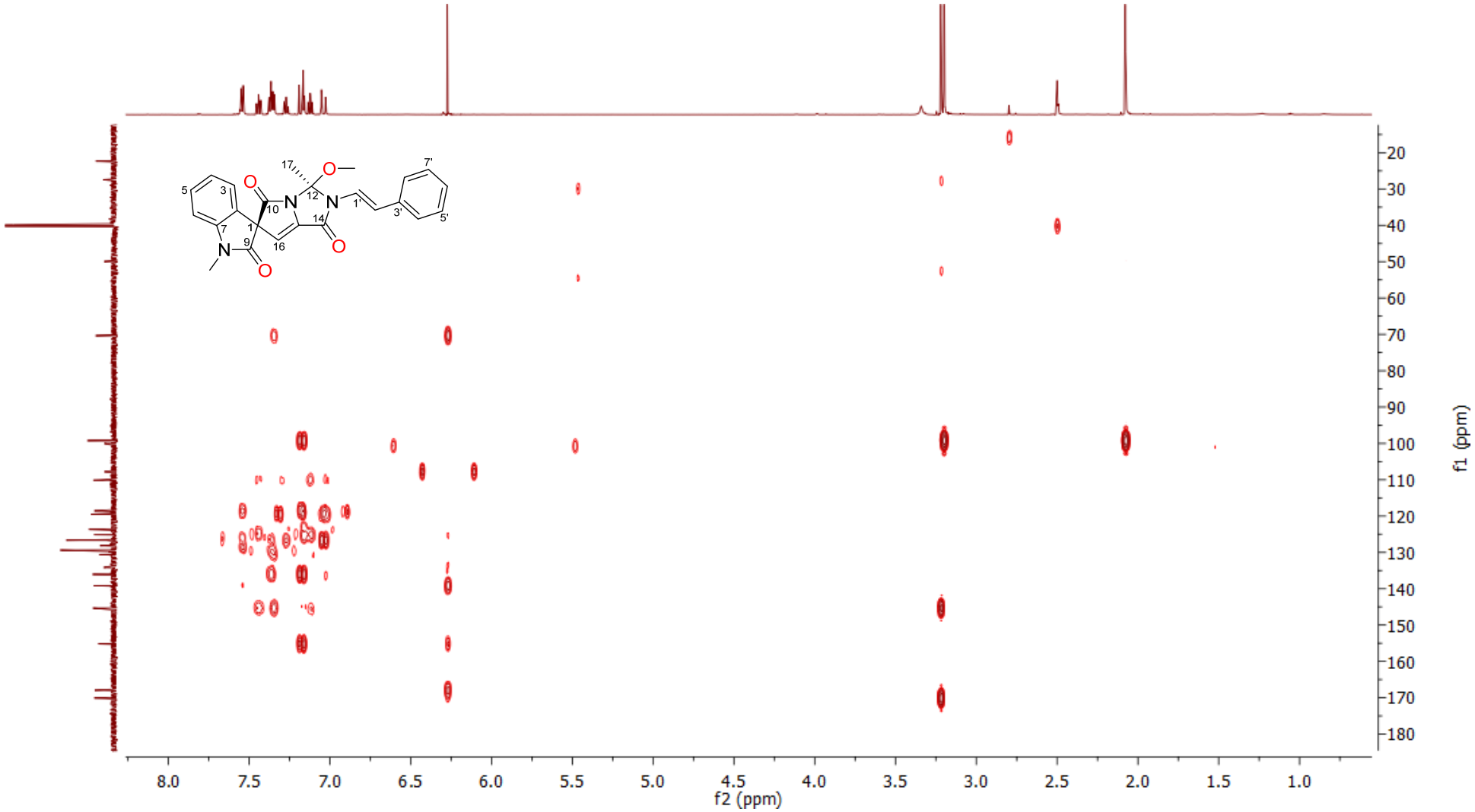

Figure S11. Expansion of HMBC spectrum of cyanogramide (**1**) in DMSO-d_6

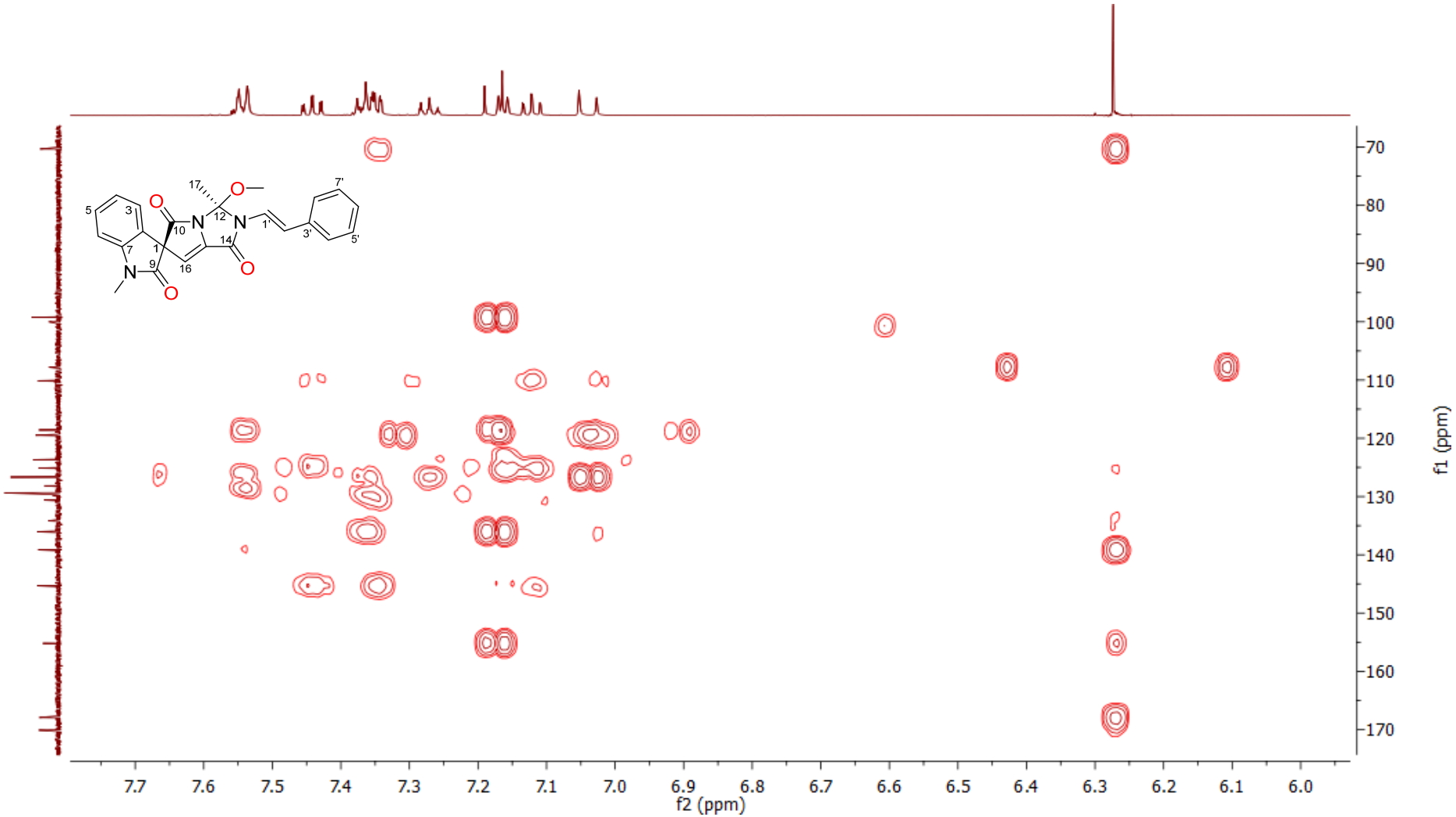

Figure S12. The NOE difference spectrum of cyanogramide (**1**) in DMSO-d_6